

A universal characteristic of type II radio bursts

E. Aguilar-Rodriguez,^{1,2,3} N. Gopalswamy,⁴ R. MacDowall,⁴ S. Yashiro,¹
and M. L. Kaiser⁴

Received 5 April 2005; revised 21 June 2005; accepted 8 July 2005; published 6 October 2005.

[1] We present a study on the spectral properties of interplanetary type II radio bursts observed by the Radio and Plasma Wave (WAVES) experiment on board the Wind spacecraft. We investigated the relative bandwidth of the type II radio bursts observed by WAVES from 1997 up to 2003. We obtained three sets of events, based on the frequency domain of occurrence: 109 events in the low-frequency domain (30 KHz to 1000 kHz, detected by the RAD1 receiver), 216 events in the high-frequency domain (1–14 MHz, observed by the RAD2 receiver), and 73 events that spanned both domains (RAD1 and RAD2). Statistical results show that the average bandwidth-to-frequency ratio (BFR) was 0.28 ± 0.15 , 0.26 ± 0.16 , and 0.32 ± 0.15 for RAD1, RAD2, and RAD1 + RAD2, respectively. We compared our results with those obtained for ISEE-3 type II bursts and found a difference in the average BFR, which seems to be due to a selection effect. The BFR of the WAVES type II bursts is similar to that of metric type II bursts reported in published works. This suggests that the BFR is a universal characteristic, irrespective of the spectral domain. Finally, we also studied the BFR evolution with heliocentric distance using white-light observation of the associated coronal mass ejections. We found that the BFR remains roughly constant in the SOHO/LASCO field of view (i.e., from 2.1 to 32 solar radii), while the bandwidth itself decreases.

Citation: Aguilar-Rodriguez, E., N. Gopalswamy, R. MacDowall, S. Yashiro, and M. L. Kaiser (2005), A universal characteristic of type II radio bursts, *J. Geophys. Res.*, *110*, A12S08, doi:10.1029/2005JA011171.

1. Introduction

[2] Solar radio bursts of type II are characterized by a narrow band of intense radiation that drifts toward lower frequencies with time. The type II solar radio bursts result from the excitation of plasma waves in the ambient medium by a shock wave propagating outward from the Sun. It is generally accepted that the radio waves are emitted near the local electron plasma frequency or its harmonics. Type II radio bursts are grouped, according to the wavelength regime in which they are observed, into metric (m), decameter/hectometric (DH), and kilometric (km) bands. While it is widely accepted that DH and km type IIs are caused by coronal mass ejection (CME) driven shocks [Sheeley *et al.*, 1985], the source is still controversial for m-type II bursts.

[3] Radio observations obtained by the Radio and Plasma Waves Experiment (WAVES) [Bougeret *et al.*, 1995] have been useful in studying type II radio bursts over a wide

range of frequencies (20 kHz to 13.85 MHz) and hence provide unique information on CMEs propagating through the entire Sun-Earth connected space. The low (RAD1) and high (RAD2) frequency receivers of the WAVES experiment record radio emission in the frequency range 20–1040 kHz and 1.075–13.825 MHz, respectively. Hundreds of type II bursts have been observed by Wind/WAVES, and their CME association has been studied [Gopalswamy *et al.*, 2001; Gopalswamy, 2004]. However, the spectral properties of type II bursts have not been studied. Since the DH wavelength range is a new regime, it is important to see how the properties of type II bursts in this range compare with metric [Mann *et al.*, 1996] and kilometric [Lengyel-Frey and Stone, 1989] regimes.

[4] An important benefit of such a comparison is a better understanding of the type II phenomenon irrespective of the wavelength domain in which the bursts are observed. In the past, only the ISEE-3 radio experiment [Knoll *et al.*, 1978] had observed a significant number of type II bursts in the interplanetary medium. The ISEE-3 radio experiment had a frequency range from 30 kHz to ~ 2 MHz. WAVES experiment has obtained a large database of type II bursts over a wider spectral range, overlapping with ISEE-3 spectral domain. While the spectral range of WAVES/RAD1 is similar to that of the ISEE-3 receiver, there is virtually no counterpart to the high-frequency WAVES receiver (RAD2).

[5] The relative instantaneous bandwidth of type II emission is related to the electron density of the medium through which the associated shock passes. The observed band-

¹Physics Department, Catholic University of America, Washington, D.C., USA.

²Now at Laboratory for Extraterrestrial Physics, NASA Goddard Space Flight Center, Greenbelt, Maryland, USA.

³Also at Instituto de Geofísica, Universidad Nacional Autónoma de México, Mexico City, Mexico.

⁴Laboratory for Extraterrestrial Physics, NASA Goddard Space Flight Center, Greenbelt, Maryland, USA.

Table 1. Type II Radio Bursts Observed by Wind/WAVES and ISEE-3 Receivers

Receiver	Frequency Range	Study Interval	Number of Events	Rate of Occurrence, events/year
RAD1	20–1040 kHz	1997–2003	109	~15.5
RAD2	1.075–13.8 MHz	1997–2003	216	~30.8
RAD1 + RAD2	20 kHz to 13.8 MHz	1997–2003	73	~10.4
ISEE-3	30–1980 kHz	1978–1983	37	–

widths of the type II spectral profiles therefore depend on the range of electron density in the radio-emitting region of the shock. *Lengyel-Frey and Stone* [1989] found that the relative instantaneous bandwidth of 33 IP type II bursts observed by ISEE-3 spacecraft ranged from 0.3 to 0.7, with an average value of 0.49 ± 0.3 . *Mann et al.* [1995] and *Mann et al.* [1996] found that the relative bandwidth of metric type II bursts ranged from 0.1 to 0.7 with the distribution peaking around 0.3. In this paper we (1) study the spectral properties of DH type II bursts, (2) study the spectral properties of the low-frequency (RAD1) type II bursts, (3) compare the spectral properties of RAD1 and RAD2 type II bursts, and (4) compare the spectral properties of WAVES type II bursts with those of the metric and ISEE-3 type II bursts.

2. Observations

[6] The WAVES experiment has several sensitive radio receivers that cover the frequency range from ~ 4 kHz to ~ 14 MHz [*Bougeret et al.*, 1995]. The receivers are connected to dipole antennas in the spacecraft spin plane and a dipole antenna along the spacecraft spin axis. Although WAVES detected type II bursts from the beginning in the kilometric (<1 MHz) domain, the DH (1–14 MHz) type II bursts started appearing only in April 1997. Early investigations concentrated on the association between type II radio bursts and CMEs [*Kaiser et al.*, 1998; *Gopalswamy et al.*, 2000, 2001; *Reiner et al.*, 2001]. Here we concentrate on the spectral properties.

2.1. Data Selection

[7] We consider all the type II bursts observed by Wind/WAVES from 1997 up to 2003. The bursts can be grouped as follows: (1) 109 events observed by RAD1 receiver (km domain), (2) 216 events recorded by the RAD2 receiver (DH domain), and (3) 73 events observed by both RAD1 and RAD2 receivers (DH-km domain). Table 1 summarizes our data set. It is necessary to point out that some events in both RAD1 and RAD2 sets have a counterpart in the DH and km domains, respectively.

[8] For comparison, we selected 37 type II events observed by the ISEE-3 radio experiment [*Cane and Stone*, 1984]. ISEE-3 was launched in August of 1978 and was placed in a halo orbit about the libration point situated approximately 240 Earth radii upstream between Earth and the Sun. ISEE-3 contained very sensitive radio receivers covering the frequency range from 30 kHz to 2 MHz in 24 channels [*Knoll et al.*, 1978]. This frequency range corresponds to radio emission in the height range from about $10 R_{\odot}$ to $215 R_{\odot}$ (1 AU) from the Sun for an undisturbed solar wind.

[9] Figure 1 shows the dynamic spectrum of a type II radio burst observed by the ISEE-3 radio experiment in

1978. The type II burst starts at ~ 1110 UT on 23 September, ending at ~ 1030 UT on 24 September, with the intense emission occurring in the frequency range ~ 700 – 110 kHz.

[10] Even though ISEE-3 had an additional channel at 1980 kHz, we have used only up to 1 MHz in order to make a correct comparison with RAD1 data. *Lengyel-Frey and Stone* [1989] used a subset of only 33 events that were well observed to study the spectral characteristics. They had reported only the average values of the distributions. Therefore we started from the original ISEE-3 data to measure the spectral properties. Even though *Cane* [1985] reported 48 events, we found it difficult to measure the spectral characteristics of 11 events. So, we do not include them in this study.

3. Data Analysis

[11] All the events in our data set were analyzed to obtain their spectral properties (bandwidth, central frequency, and flux density relative to the cosmic background) in the dynamic spectrum. In order to analyze each type II burst, we used a technique which isolates the type II event from the dynamic spectrum by setting to zero any emission outside the type II burst feature. We used this reduced dynamic spectrum to measure the spectral properties. From these measurements we perform a statistical analysis of the spectral characteristics of type II bursts.

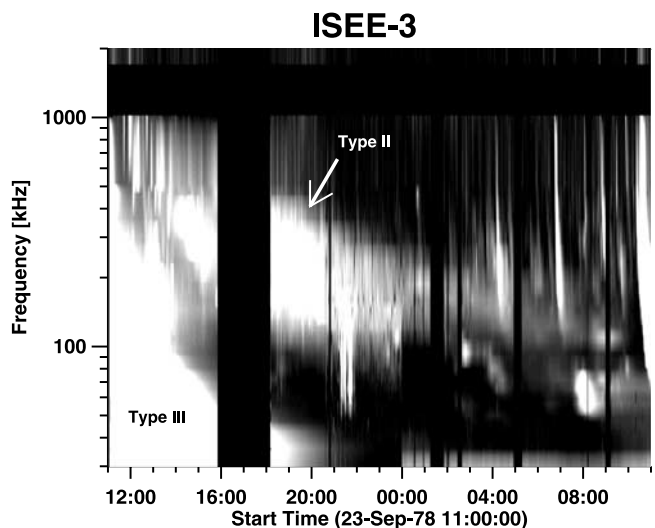


Figure 1. Dynamic spectrum of a type II radio burst observed by the ISEE-3 radio experiment in 1978. Type II emission starts at ~ 1110 UT on 23 September, ending at ~ 1030 UT on 24 September. Most of the intense emission is observed from the beginning of the event at ~ 700 kHz until around 0100 UT on 24 September at ~ 110 kHz. See color version of this figure in the HTML.

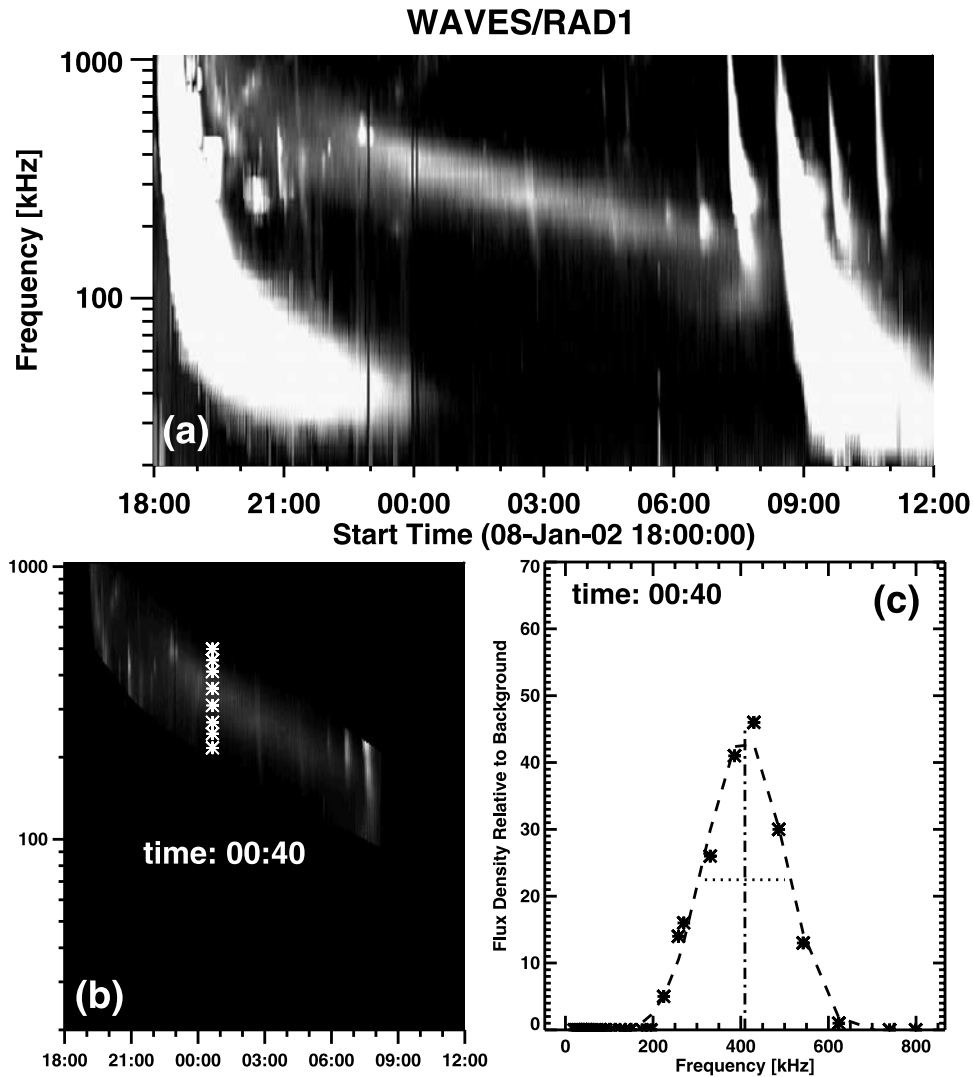


Figure 2. Method to obtain spectral properties of a type II radio burst. (a) Type II burst dynamic spectrum. (b) The type II burst is isolated from the dynamic spectrum by setting to zero any emission outside the type II feature. (c) Profile of the flux density (relative to the cosmic background) versus the observed frequency (asterisks) obtained at the time 0040 UT (asterisks). Dashed line indicates the gaussian fit of the profile. Dash-dotted line indicates the central frequency at the profile peak and the dotted line indicates the full width at a half maximum of the profile. See color version of this figure in the HTML.

[12] Figure 2 illustrates the technique. On 8 January 2002, WAVES/RAD1 receiver detected a type II radio burst starting at ~ 1830 UT at 1 MHz and drifting down to 100 kHz at ~ 0830 UT on 9 January (Figure 2a). Figure 2b shows the type II burst isolated from the dynamic spectrum and a cut in time (0040 UT) for spectral measurements by plotting the flux density as a function of the observing frequency. Figure 2c shows the flux density versus the frequency of the type II radio burst at the time 0040 UT (asterisks), with the gaussian fit to the profile (dashed line). The central frequency (dash-dotted line) at the profile peak and the full width at a half maximum (dotted line) of the profile are also shown.

3.1. Bandwidth-to-Frequency Ratio

[13] The measurements of spectral properties of the type II bursts are carried out as follows. The duration

of a type II event is divided into n equal intervals of 60 s, i.e., $t_{j+1} - t_j = 60$ s. At each time t_j we obtain a profile of the flux density as a function of the observed frequency as illustrated in Figure 2. The flux density is relative to the cosmic background. We fit a gaussian to this profile to compute (1) the peak of the flux density, (2) the central frequency (f_j), and (3) the full width at half maximum of the profile (Δf_j). The instantaneous relative bandwidth (IRB) at time t_j is given by

$$IRB = \frac{\Delta f_j}{f_j}. \quad (1)$$

Averaging over all t_j s, we find the mean value of the instantaneous relative bandwidth of a type II burst. Here-

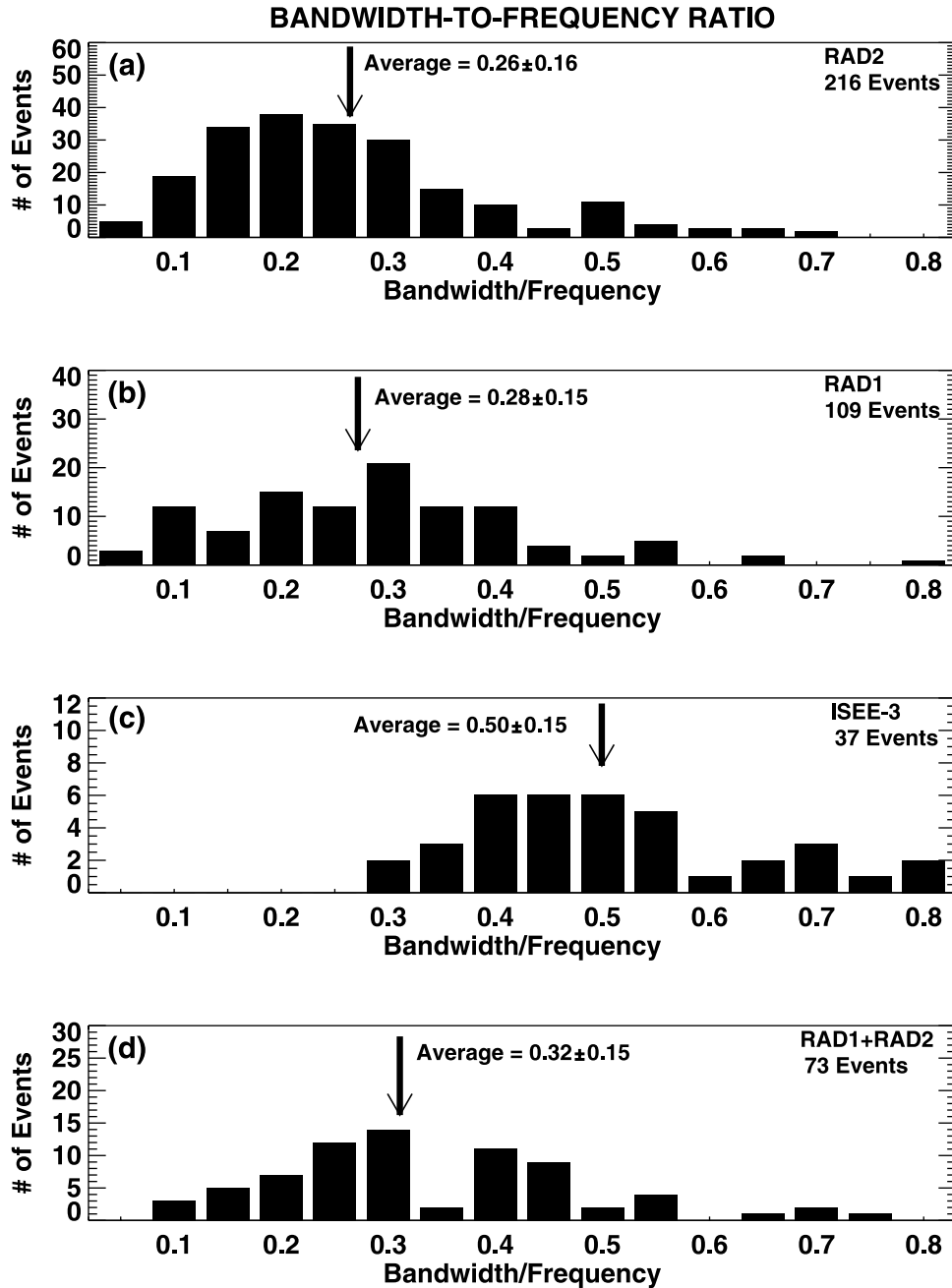


Figure 3. BFR histograms for type II solar radio bursts detected by (a) RAD2, (b) RAD1, (c) ISEE-3, and (d) RAD1 + RAD2 receivers.

after, this mean value is referred to as the bandwidth-to-frequency ratio (BFR) and is given by

$$BFR = \frac{1}{n} \sum_{j=1}^n \frac{\Delta f_j}{f_j}. \quad (2)$$

Lengyel-Frey and Stone [1989] analyzed type II spectral profiles, plotted as log of flux density in solar flux units versus log of the observed frequency, computed from 30-min averages of ISEE-3 radio data. They measured several parameters which characterize the type II spectral profiles (1) log of peak flux density, (2) log of integrated flux density,

and (3) bandwidth-to-frequency ratio, where the bandwidth is the full width at half maximum of the profile. We measured these parameters by applying the technique described above to obtain the BFR of type II radio bursts observed by Wind/WAVES and ISEE-3. As in the *Lengyel-Frey and Stone* [1989] study, our study of type II spectral profiles is dependent on factors such as the duration and flux density of the event emission, gaps in the data coverage as well as contamination from other sources of emission, such as type III bursts.

[14] Figure 3 shows, from the top to the bottom, the BFR distributions for type II bursts in the RAD2, RAD1, RAD1 + RAD2, and ISEE-3 spectral domains. The

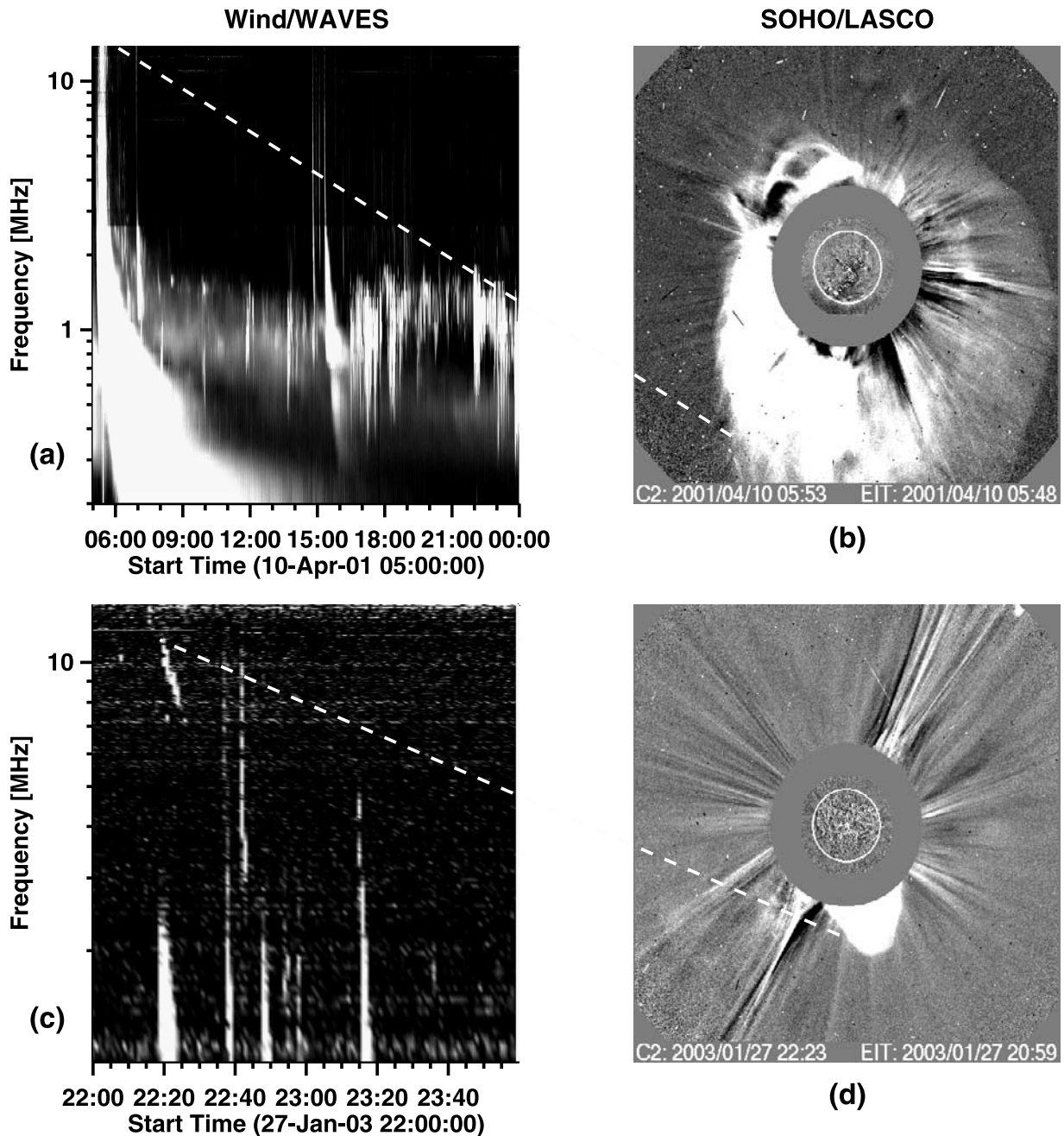


Figure 4. Examples of type II radio bursts (observed by Wind/WAVES) and their associated CMEs (observed by SOHO/LASCO) for which we computed the BFR. (a) Shows a type II burst drifting from 14 MHz to ~ 100 kHz and (b) was associated with a fast (2411 km/s) halo CME. The BFR obtained for this event was 0.51. (c) Shows a brief type II burst drifting from 11 MHz to 8 MHz, which was associated with a fast (1053 km/s) CME, and (d) an eruptive filament. For this event we obtained a BFR = 0.13. See color version of this figure in the HTML.

corresponding number of events and the average values of the distributions with standard deviation are also noted in the figure. Figure 3a shows the BFR histogram for the 216 type II bursts observed by the RAD2 receiver, 73 of which had counterparts in RAD1. The distribution lies in the interval $0.05 \leq \text{BFR} \leq 0.7$. The BFR averaged over 216 events is $\langle \text{BFR} \rangle = 0.26 \pm 0.16$, which is the lowest BFR value compared to all other distributions. Both ISEE-3 and RAD1 detect type II radio bursts in the kilometric domain. Figure 3b shows the BFR distribution for the 109 events

observed by RAD1, 73 of which had counterparts in RAD2. The distribution lies in the interval $0.05 \leq \text{BFR} \leq 0.8$ with an average BFR of $\langle \text{BFR} \rangle = 0.28 \pm 0.15$. Figure 3c shows the BFR histogram for the 37 type IIs observed by ISEE-3. The BFR ranges from 0.3 to 0.8, with an average value of 0.5 ± 0.15 . For a subset of these ISEE-3 bursts, *Lengyel-Frey and Stone* [1989] obtained $\langle \text{BFR} \rangle = 0.49 \pm 0.3$, which is in agreement with our study.

[15] Type II radio bursts detected by RAD1 + RAD2 receivers are the most energetic because the associated

shock propagates through the entire Sun-Earth distance. Their BFR distribution (Figure 3d) lies in the interval $0.1 \leq \text{BFR} \leq 0.75$. The BFR averaged over 73 events is $\langle \text{BFR} \rangle = 0.32 \pm 0.15$.

3.2. CMEs and IP Type II Radio Bursts

[16] As mentioned in the introduction section, there is a close relationship between CME-driven shocks and IP type II radio bursts. Both CMEs and IP type II radio-bursts continue to be observed by SOHO/LASCO and Wind/WAVES, respectively. Moreover, the fact that these spacecraft have overlapping observations during our study period allows us to relate type II spectral characteristics with the CME properties.

[17] We investigated the evolution of the bandwidth and BFR with the heliocentric distance for type II radio bursts. Since the DH spectral domain corresponds to plasma frequencies within the field of view of the SOHO/LASCO coronagraphs, it is possible to infer the heliocentric distance of the type II burst in the DH domain by measuring the heliocentric distance of the associated white-light CME [Gopalswamy *et al.*, 2001].

[18] Figure 4 shows two Wind/WAVES type II radio bursts and their associated CMEs. In the first case, the type II burst was observed between ~ 0524 and ~ 2400 UT on 10 April 2001 (see Figure 4a), drifting from 14 MHz to ~ 100 kHz. The type II burst was associated with a fast halo CME (see Figure 4b) that had a plane of the sky speed of 2411 km/s. The CME was associated with an intense flare (X2.3) from active region 9415 (S23W09) starting at 0506 UT. The BFR for this type II burst was 0.51. Figure 4c shows the second type II burst on 27 January 2003. This is a brief event, starting at ~ 2220 UT at ~ 11 MHz and ending at ~ 2226 UT at ~ 8 MHz. The associated CME was also fast (see Figure 4d), with a sky-plane speed of 1053 km/s measured at a position angle of 205. The CME was associated with a C2.4 flare from active region 9415 (S17W23) starting at 2142 UT. The type II burst had a BFR = 0.13, which is significantly lower than that obtained for the first case.

[19] For each of the CME-type II burst pairs, we obtained the time and the corresponding heliocentric distance measurements of the CME as it moved away from the Sun. The time resolution of the radio observations varied from 16 s for RAD2 and 1 min for RAD1. The time resolution of the white light observation was much poorer because the typical cadence is ~ 30 min. We extrapolated the CME times when the observing times did not match those of the radio burst [Yashiro *et al.*, 2004]. Then, by matching the CME times with those of the type II burst, we were able to show how the bandwidth and the BFR (measured from the spectral profiles) evolve with the heliocentric distance. The shock is expected to be at the standoff distance from the CME [Gopalswamy *et al.*, 2005]. This distance is expected to be small near the Sun, so we assume that the front shock, which produces the type II emission, is very close to the leading edge of the CME. Certainly, such an assumption is affected by factors such as (1) the actual height of the type II burst is likely to be smaller than the height of the CME leading edge if the type II burst is formed at the flanks of the shock where the condition for electron acceleration is known to be favorable [Holman and Pesses, 1983], and

(2) the projection effects, which make the measured plan-of-sky distance smaller for halo CMEs than the actual distance. For limb events the CME height represents an upper limit for the type II height. For disk events (halo CMEs), the CME height can be taken as a lower limit to the type II height. A combination of these two effects may be responsible for the large scatter in Figure 5. However, as a first approximation, combined radio and white-light observations represent a useful tool to be used.

[20] To analyze the evolution of bandwidth and BFR with the heliocentric distance, we considered only the 73 events which spanned both RAD1 and RAD2 receivers (i.e., RAD1 + RAD2). Owing to SOHO/LASCO data gaps, we had to drop several events resulting in a set of 66 type II bursts with SOHO/LASCO observations. We were able to identify a unique white-light CME for each one of these type II bursts.

[21] Figure 5a shows the bandwidth (Δf) evolution with respect to the heliocentric distance for the 66 RAD1 + RAD2 type II events. We see a clear anticorrelation between the bandwidth and heliocentric distance ($r = 0.51$). Near the Sun, the average Δf is ~ 630 kHz; far away it is $\Delta f \sim 80$ kHz. Lengyel-Frey and Stone [1989] found Δf decreasing from ~ 320 to ~ 20 kHz for the ISEE-3 type IIs. However, it is important to mention that the difference between the two results is the way in which the heliocentric distance was determined. In our study, the heliocentric distance was determined using the time from the spectrum and the corresponding distance from the CME height-time plot. This explains why our heliocentric distance range is restricted to the LASCO-C2-C3 field of view (i.e., from 2.1 to 32 solar radii). Lengyel-Frey and Stone [1989] used the time of the spectrum and the average shock transit speed given by Cane [1985] to obtain the heliocentric distance range (0.05 to 1 AU). By considering the overlapping heliocentric distance for WAVES and ISEE-3, which is from ~ 0.05 to ~ 0.14 AU, Δf decreases from ~ 320 to ~ 125 kHz and from ~ 316 to ~ 80 kHz for ISEE-3 and WAVES, respectively. This is an excellent agreement. Figure 5b shows the BFR evolution with the heliocentric distance for the 66 RAD1 + RAD2 type II events. The plot shows that the BFR of type II events has only a weak correlation with the heliocentric distance ($r = 0.24$). This point is also in agreement with the Lengyel-Frey and Stone [1989] study. A least squares fit to the data gives $\text{BFR} = 0.23(\pm 0.001) + 1.62(\pm 0.014)R$, where R is the heliocentric distance.

4. Discussion

[22] We analyzed the spectral properties of type II radio bursts observed by Wind/WAVES and compared them with previous results for type IIs in the metric [Mann *et al.*, 1995; Mann *et al.*, 1996] and kilometric [Lengyel-Frey *et al.*, 1985; Lengyel-Frey and Stone, 1989] domains. The present study closes the gap between the metric and km domains and permits us to compare the BFR distributions in different domains. Since Wind/WAVES also observes type IIs in the kilometric domain, we were able to compare the type II properties from ISEE-3 observations.

[23] Type II bursts observed in the DH domain (WAVES/RAD2) have an average BFR of 0.26 ± 0.16 , whereas those observed at kilometric wavelengths (WAVES/RAD1) have

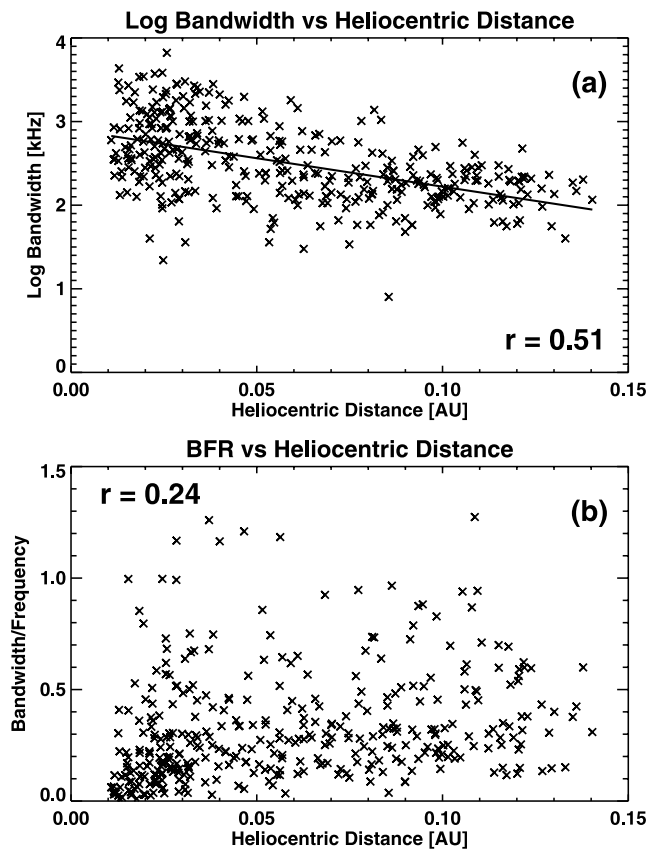


Figure 5. (a) Plot showing the change of bandwidth with heliocentric distance for 66 type II events that spanned the RAD1 and RAD2 spectral domains. (b) BFR of type II radio bursts do not show correlation with the heliocentric distance.

an average BFR of 0.28 ± 0.15 . The difference is not significant. Some type II bursts observed by RAD1 and RAD2 have a counterpart type II emission at DH and km domains, respectively. The average BFR for those type IIs which spanned both DH and km domains is 0.32 ± 0.15 , which is practically the same as that obtained by *Mann et al.* [1996] in the metric domain (0.32 ± 0.14). By isolating the type IIs without counterparts, we obtained two subsets of purely DH and km type IIs, respectively. Figure 6 shows the BFR distributions for these subsets. We found an average BFR of 0.23 ± 0.13 and 0.26 ± 0.11 for the DH and km domains, respectively. These average values do not differ significantly (less than $\sim 12\%$) from those obtained for the complete RAD1 and RAD2 sets.

[24] *Lengyel-Frey and Stone* [1985] found an average BFR of 0.49 ± 0.3 for ISEE-3 type II bursts. When we reanalyzed the ISEE-3 data, we found an average BFR of 0.50 ± 0.15 , which is virtually equal to that obtained by *Lengyel-Frey and Stone* [1985]. This is somewhat puzzling because the BFR is a factor 2 higher for the ISEE-3 events compared to the RAD1 events. Both WAVES/RAD1 and ISEE-3 receivers have similar frequency coverage. As we mentioned in section 1, we used ISEE-3 data only up 1 MHz in order to make a comparison with the RAD1 receiver. The difference seems to be due to different spectral resolution of

RAD1 and ISEE-3 receivers. The differences between these results could also be due to the fact that we considered not only RAD1 events with high-frequency counterparts but also events confined to the RAD1 spectral domain, whereas such a correspondence is unknown for the ISEE-3 list.

[25] We now consider the spectral coverage of ISEE-3 and RAD1 receivers. Table 2 shows the frequency channels for RAD1 and ISEE-3 receivers. We see that the ISEE-3 frequencies are not log-spaced and the number of channels above 400–500 kHz is less than that for RAD1 receiver. Thus bursts with smaller Δf can easily be missed in the spectral domain with sparse channels. This can be clearly seen in Figure 3c: The ISEE-3 distribution does not have BFR values less than 0.3, whereas the RAD1 distribution has many events with BFR values less than 0.3. This deficiency in the ISEE-3 distribution makes the average value to be higher. Therefore the difference between the average of ISEE-3 and RAD1 distributions is likely due to selection effect. This is consistent with the fact that *Lengyel-Frey and Stone* [1989] ignored many small events.

[26] In order to see the effect of channel spacing, we analyzed 28 type II bursts observed by both RAD1 and the Thermal Noise Receiver (TNR), which is also on board the Wind spacecraft. The TNR has a frequency range of 4–256 kHz in five logarithmically spaced frequency bands [*Bougeret et al.*, 1995]. Each of these bands is divided into either 32 or 16 logarithmically spaced channels. Hence

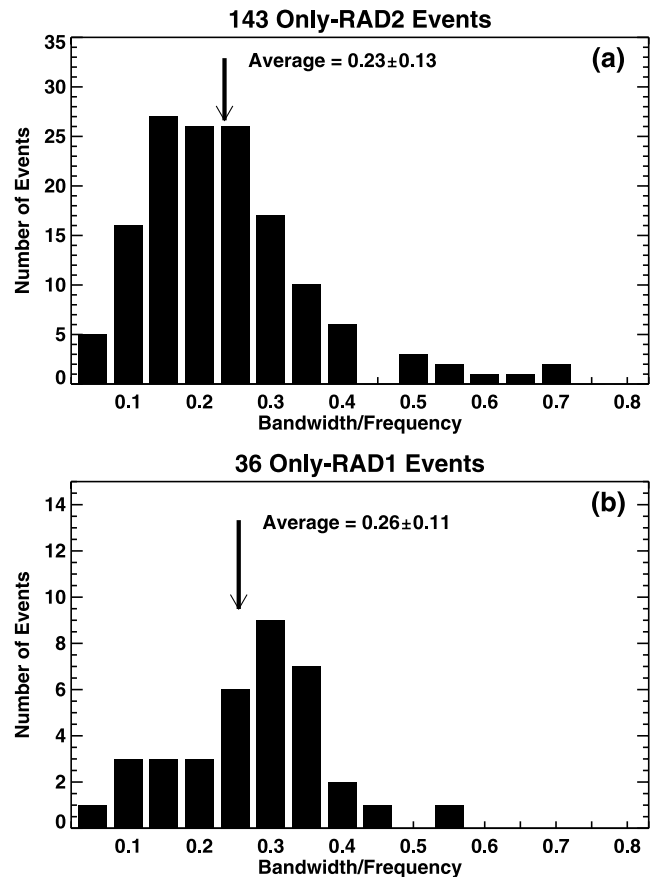


Figure 6. BFR distributions for type II radio burst observed by (a) RAD2 and (b) RAD1 receivers without counterpart emission.

Table 2. ISEE-3 and RAD1 Observing Frequencies in kHz^a

Frequency Number	ISEE-3	RAD1
1	41	20
2	50	24
3	60	28
4	72	32
5	94	36
6	123	40
7	160	44
8	233	48
9	360	52
10	513	60
11	1000	72
12	1980	80
13	30	92
14	36	104
15	47	124
16	56	136
17	66	148
18	80	176
19	110	196
20	145	224
21	188	256
22	290	272
23	466	332
24	1000	388
25		428
26		484
27		540
28		624
29		740
30		804
31		940
32		1036

^aISEE-3 receiver has 3 kHz bandwidths for frequency numbers 1 to 12, and 10 kHz bandwidths for frequency numbers 13 to 24.

TNR has a much better frequency resolution compared to the RAD1 receiver. Figure 7a shows the BFR distribution of the 28 type IIs observed by RAD1 below 250 kHz. The range is from 0.15 to 0.55, with an average of 0.35 ± 0.10 . Figure 7b shows the BFR distribution for the same events, but observed by TNR, which lies in the interval $0.05 \leq \text{BFR} \leq 0.6$, with an average of 0.30 ± 0.14 . Therefore the channel spacing in ISEE-3 receiver leads to an overestimate of the BFR, which is more pronounced at the high end and the low end of the ISEE-3 frequency range. The same also applies for RAD1, even using just the measured channels, albeit to a lesser extent than for ISEE-3. However, for RAD2 receiver, our results are not limited to this effect because there is no interpolation between their channels.

[27] Table 3 summarizes the average BFR for all the type II bursts observed by Wind/WAVES and ISEE-3 receivers. If we account for the fact that the channel spacing in RAD1 and ISEE-3 receivers leads to an overestimate of the BFR, we can conclude that the BFR is a universal characteristic in both DH and km regimes.

[28] *Mann et al.* [1996] obtained a BFR value of 0.32 ± 0.14 in the metric domain. However, in their study the BFR is defined to the low-frequency edge of the type II bursts, whereas in our study we determined the BFR with respect to the central frequency of the emission. By computing the BFR using the *Mann et al.* [1996] definition, we found an average BFR of 0.35 ± 0.25 and 0.35 ± 0.24 for those type IIs observed in the km and DH domains, respectively. This is in agreement with the *Mann et al.* [1996] study. Therefore

we see that the BFR is a universal property over the entire Sun-Earth connected space. As pointed out by *Lengyel-Frey and Stone* [1989], the observed type II bandwidths and BFR reflect the properties of the large-scale electron density distribution. In the same way, they mention that the average $\Delta n/n$ ratio (where Δn is the size of the density fluctuations which produce a spectrum of bandwidth Δf and where $\Delta f/f = 1/2 \Delta n/n$) is relatively constant over the range of the type II observations, as indicated by the relative constancy of the observed BFR with the distance. Figure 5b shows the lack of correlation between BFR and heliocentric distance, which implies that $\Delta n/n$ is also independent of the distance, as pointed out by *Lengyel-Frey and Stone* [1989]. Other studies have analyzed the BFR at different wavelengths and their corresponding implications with the shock evolution from near to the Sun to 1 AU [*Vrsnak et al.*, 2001, 2002, 2003]. The fact that the average BFR results to be roughly constant over the different wavelength regimes suggests that the density fluctuation structure of the medium is on average the same, irrespective of the spectral domain.

5. Conclusions

[29] We have analyzed the radio emission properties of type II radio bursts observed by the WAVES radio exper-

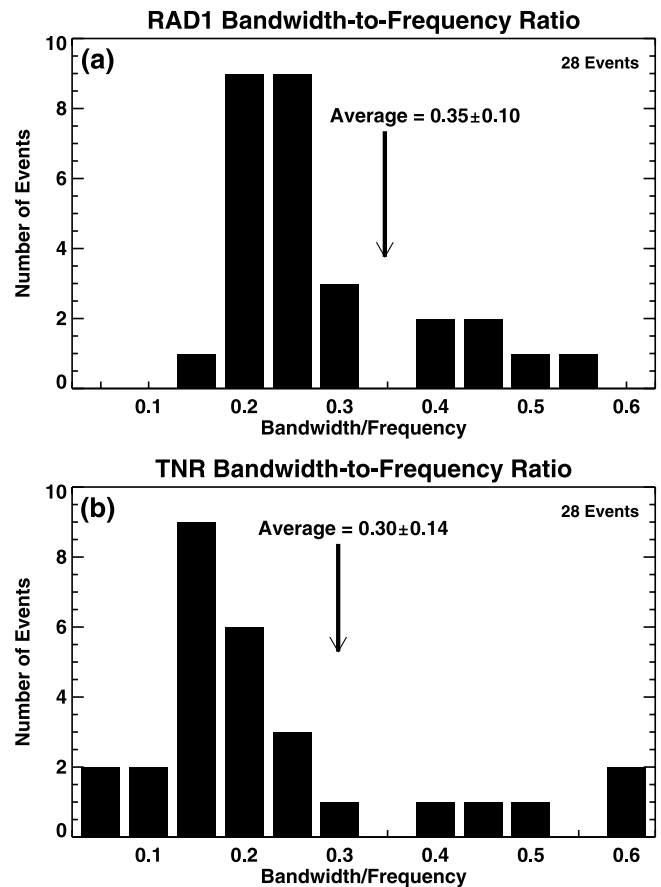


Figure 7. BFR distributions for 28 type II radio burst observed by (a) RAD1 and (b) TNR receivers below 250 kHz. The difference in the BFR average values is due to the fact that the channel spacing in RAD1 receiver leads to an overestimate of the BFR.

Table 3. Average BFR for Type II Radio Bursts Observed by Wind/WAVES and ISEE-3 Receivers

Receiver	Number of Events	Average BFR
RAD2	216	0.26 ± 0.16
RAD1	109	0.28 ± 0.15
ISEE-3	37	0.50 ± 0.15^a
ISEE-3	33	0.49 ± 0.30^b
RAD1 + RAD2	73	0.32 ± 0.15
TNR ^c	28	0.30 ± 0.14
RAD1 ^c	28	0.35 ± 0.10

^aPresent study.^bLengyel-Frey and Stone [1989].^cEvents analyzed below 250 kHz.

iment from 1997 up to 2003 and their association with white-light CMEs observed by the SOHO/LASCO coronagraphs. We compared our results with those obtained by Lengyel-Frey and Stone [1989] (km domain) and Mann *et al.* [1996] (metric domain). Our study shows that (1) the bandwidth-to-frequency ratio is a universal characteristic of the type II radio bursts, irrespective of the spectral domain, (2) the bandwidth is anticorrelated with the heliocentric distance, and (3) the bandwidth-to-frequency ratio has no correlation with the heliocentric distance.

[30] **Acknowledgments.** The SOHO/LASCO data used here are produced by a consortium of the Naval Research Laboratory (USA), Max-Planck-Institut für Aeronomie (Germany), Laboratoire d'Astronomie (France), and the University of Birmingham (UK). SOHO is a project of international cooperation between ESA and NASA. The authors also thank the referees for the comments that have improved this manuscript.

[31] Shadia Rifai Habbal thanks Munetoshi Tokumaru and Gottfried Mann for their assistance in evaluating this paper.

References

- Bougeret, J. L., et al. (1995), Waves: The radio and plasma wave investigation on the Wind spacecraft, *Space Sci. Rev.*, *71*, 231.
- Cane, H. V. (1985), The evolution of interplanetary shocks, *J. Geophys. Res.*, *90*, 191.
- Cane, H. V., and R. G. Stone (1984), Type II solar radio bursts, interplanetary shocks, and energetic particle events, *Astrophys. J.*, *282*, 339.
- Gopalswamy, N. (2004), Recent advances in the long-wavelength radio physics of the Sun, *Planet. Space Sci.*, *52*, 1399.
- Gopalswamy, N., M. L. Kaiser, B. J. Thompson, L. F. Burlaga, A. Szabo, A. Vourlidas, A. Lara, S. Yashiro, and J. L. Bougeret (2000), Radio-rich solar eruptive events, *Geophys. Res. Lett.*, *27*, 1427.

- Gopalswamy, N., S. Yashiro, M. L. Kaiser, R. A. Howard, and J. L. Bougeret (2001), Characteristics of coronal mass ejections associated with long-wavelength type II radio bursts, *J. Geophys. Res.*, *106*, 29,219.
- Gopalswamy, N., E. Aguilar-Rodriguez, S. Yashiro, S. Nunes, M. L. Kaiser, and R. A. Howard (2005), Type II radio bursts and energetic solar eruptions, *J. Geophys. Res.*, doi:10.1029/2005JA011158, in press.
- Holman, G. D., and M. E. Pesses (1983), Solar type II radio emission and the shock drift acceleration of electrons, *Astrophys. J.*, *267*, 837.
- Kaiser, M. L., M. J. Reiner, N. Gopalswamy, R. A. Howard, O. C. St Cyr, B. J. Thompson, and J.-L. Bougeret (1998), Type II radio emissions in the frequency range from 1–14 MHz associated with the April 7, 1997 solar event, *Geophys. Res. Lett.*, *25*, 2501.
- Knoll, R., et al. (1978), The 3-dimensional radio mapping experiment (SBH) on ISEE-C, *IEEE Trans. Geosci. Electron.*, *GE-16*, 199.
- Lengyel-Frey, D., and R. G. Stone (1989), Characteristics of interplanetary type II radio emission and the relationship to shock and plasma properties, *J. Geophys. Res.*, *94*, 159.
- Lengyel-Frey, D., R. G. Stone, and J. L. Bougeret (1985), Fundamental and harmonic emission in interplanetary Type II radio bursts, *Astron. Astrophys.*, *151*, 215.
- Mann, G., T. Classen, and H. Aurass (1995), Characteristics of coronal shock waves and solar type II radio bursts, *Astron. Astrophys.*, *295*, 775.
- Mann, G., A. Klassen, H. T. Classen, H. Aurass, D. Scholz, R. J. MacDowall, and R. G. Stone (1996), Catalogue of solar type II radio bursts observed from September 1990 to December 1993 and their statistical analysis, *Astron. Astrophys. Suppl.*, *119*, 489.
- Reiner, M. J., M. L. Kaiser, and J. L. Bougeret (2001), Radio signatures of the origin and propagation of coronal mass ejections through the solar corona and interplanetary medium, *J. Geophys. Res.*, *106*, 29,989.
- Sheeley, N. R., et al. (1985), Coronal mass ejections and interplanetary shocks, *J. Geophys. Res.*, *90*, 163.
- Vrsnak, B., et al. (2001), Band-splitting of coronal and interplanetary type II bursts. I. Basic properties, *Astron. Astrophys.*, *377*, 321.
- Vrsnak, B., et al. (2002), Band-splitting of coronal and interplanetary type II bursts. II. Coronal magnetic field and Alfvén velocity, *Astron. Astrophys.*, *396*, 673.
- Vrsnak, B., et al. (2003), Band-splitting of coronal and interplanetary type II bursts. III. Physical conditions in the upper corona and interplanetary space, *Astron. Astrophys.*, *413*, 753.
- Yashiro, S., N. Gopalswamy, G. Michalek, O. C. St. Cyr, S. P. Plunkett, N. B. Rich, and R. A. Howard (2004), A catalog of white light coronal mass ejections observed by the SOHO spacecraft, *J. Geophys. Res.*, *109*, A07105, doi:10.1029/2003JA010282.

E. Aguilar-Rodriguez and S. Yashiro, Physics Department, Catholic University of America, Washington, DC 20064, USA. (ernesto@ssedmail.gsfc.nasa.gov)

N. Gopalswamy, R. MacDowall, and M. L. Kaiser, Laboratory for Extraterrestrial Physics, NASA Goddard Space Flight Center, Code 695.0, Greenbelt, MD 20771, USA.